EXPERIMENTAL STUDY OF THE SUPERCONDUCTING MICROSTRIP ANTENNA AS A PROTECTIVE DEVICE OF THE RECEIVER FROM ELECTROMAGNETIC DAMAGE

Oleksandr Fyk
Department of Informatics and Information Technologies
National Academy of the National Guard of Ukraine
3 Zakhysnykiv Ukrainy sq., Kharkiv, Ukraine, 61001
aifleks@ukr.net

Dmutro Kucher
Department of Armament, Communications and Automated Control Systems
Institute of Naval Forces
National University «Odesa Maritime Academy»
8 Didrikhson str., Odessa, Ukraine, 65029
dima_kucher@i.ua

Roman Gonchar
Department of operation and repair of cars and military vehicles
National Academy of the National Guard of Ukraine
3 Zakhysnykiv Ukrainy sq., Kharkiv, Ukraine, 61001
Ganga1517@ukr.net

Abstract

The paper presents the results of experimental studies of a superconducting protective antenna, which consists of a high-temperature film deposited by a magnetron or a laser beam on a substrate. The work is carried out:

− analysis of the selection criteria for the substrate type (Al_2O_3, Y_2O_3, $SrTiO_3$, MgO) and the method for depositing a high-temperature superconducting film (HTSF) on its surface – YBaCuO

− analysis of the methods of making contacts, which allow to reduce losses when passing a signal from the superconducting microstrip antenna to the waveguide path.

The aim of this article is determination of the parameters of a prototype sample of a microstrip antenna device made from HTSF: transient characteristics of high-temperature superconductors, HTSF impulsive characteristics, recovery time of the superconducting state after the action of a powerful pulse on the protective device, the amplitude-frequency characteristics of the protective device in the superconducting state. This will allow to evaluate the possibility of using a microstrip antenna device made from high-temperature superconductors to protect the receiving systems from electromagnetic damage. The absence of a unified theory of high-temperature superconductivity leads to the need to select an analytical form of the functions of the amplitude-frequency characteristics of superconducting protection, and for this mathematical models are used in the programs "APPROX", "MathCAD14.0". The reliability of the obtained results of mathematical modeling of the processes of protection and recovery of the superconducting state after electromagnetic shock are confirmed in the course of experimental studies (an error of 0.15 %).

Keywords: high-temperature superconducting film, microstrip antenna, protective device, magnetron sputtering systems, coefficient of thermal expansion.

DOI: 10.21303/2461-4262.2017.00436

1. Introduction

Numerous studies have shown that an electromagnetic pulse (energy-10^3–10^8 J, duration 10^{-6}–10^{-12} s), which disables the radioelectronic equipment of radio engineering systems, is formed using the existing methods of generating powerful electromagnetic influences used in the basis of electromagnetic weapons.

The response time of existing types of protective devices, with the exception of the superconducting microstrip memory, is longer than the duration of the electromagnetic pulse, and therefore they do not allow reliable protection of the radioelectronic equipment (REE) from penetrating the EMR into the receiver.

And the most promising is the use as a protection of high-temperature superconductors, the response time of which is much smaller than the EMR front of any nature. Studies [1] have shown that electromagnetic suppression or damage occurs through the antenna-feeder path (i. e., when an electromagnetic wave passes through the receiving band of a vulnerable radio equipment). Therefore, it is actual to carry out experimental studies of the microstrip superconducting antenna protection of a receiver from electromagnetic damage. To solve this problem, it is necessary to justify everything starting from the method of manufacturing the superconducting antenna, ending with the measurement circuits and methods with the necessary list of measuring devices.

2. Materials and methods

A thin-film technology based on magnetron sputtering, thermal sputtering using electron beams, and a variety of special techniques, such as photolithography, scribing and microwelding, are used to create a high-temperature superconductor.

When testing prototype models of protective devices, the following devices are used: pulse shaper И1-7; power supply Б5-50; oscilloscope С7-13 (PA named after V. Lenin, Belarus, Minsk), С8-14 ("Izmeritel" factory, Armenia, Abovyan city); measuring instrument Р4-11 (PA named after 60th Anniversary of October, Lithuania, Vilnius); generator Г 3-34 (Nizhny Novgorod plant named after M. Frunze).

The measurements, the results of which are given in the work, are carried out in the study of a prototype of a superconducting protective microstrip antenna – HTSF – film ($YBa_2Cu_3O_7$) 0.1 μm thick deposited using the magnetron method on a substrate ($LaAlO_3$). Contact of HTSF from the residential coaxial cable (PK-75) is carried out using vacuum or magnetron sputtered gold on a part of the film in contact with the holder.

2. 1. Selection of the substrate for the superconducting microstrip element

The choice of materials for substrates is one of the main questions that form the superconducting properties of HTSFs. There are four main factors influencing the substrate material or the rewinding layer on the parameters and characteristics of the HTSF [3, 4–8].

1. Chemical reactions in the boundary (interferential) region between the HTSF and the substrate. The products of these reactions as a result of contamination of the HTSFs by new phases can cause loss of superconducting properties in the film, and the release of copper from HTSF (YBaCuO) enters silicon and can substantially change its electrophysical properties.

2. Mechanical stresses between the film and the substrate. These stresses can reach a significant value due to the difference in the coefficient of thermal expansion (CTE) of the HTSF and the substrate. For example, CTE of YBaCuO film, depending on the oxygen content and the change in phase transitions during thermal cycling, is in the range (8.5–15) 10^{-6} 1/K, while the CTE of the most frequently used substrates is, respectively, Al_2O_3–5: stabilized Y_2O_3–7; $SrTiO_3$–9,4; MgO–13–10^{-6} 1/K.

3. Orientation of crystallites. The best parameters of HTSFs are obtained with a high epitaxial orientation of the crystallites or in single-crystal films. For example, the parameters of the $LaAlO_3$ lattice (0.379 nm) agree with an accuracy of 1 % with the corresponding parameter for YBaCuO (the crystal lattice structure is shown in **Fig. 1**).

4. The magnitude of the dielectric constant and the dielectric loss of the substrate material. For example, for the microwave, the substrates used in $SrTiO_3$ are unsuitable because they have a very high dielectric permittivity (ε=100, 1000 and 18000 at T = 300.77 and 4.2 K, respectively [3, 6]) and significant dielectric losses at the microwave tgδ=5×10^{-6} and 9×10^{-6} respectively). Significantly lower losses on microwave have substrates (**Table 1**) from lanthanum aluminate $LaAlO_3$ (ε–15 at f=1 kHz and 26 at f = 0.1-1 THz, tgδ = 6×10^{-4} (300 K) and 5×10^{-6} (4 K)) [3].

The criteria for choosing the substrate are not unambiguous. On the one hand, it is desirable to have substrates with a certain crystal structure that allows for the epitaxial growth of the HTSFs, but on the other hand, it is necessary to apply films to widely used materials (silicon, silicon oxide, gallium arsenide, etc.). **Table 1** shows a qualitative comparison of the suitability of the most common types of substrates for the deposition of HTSFs [3, 4, 8].

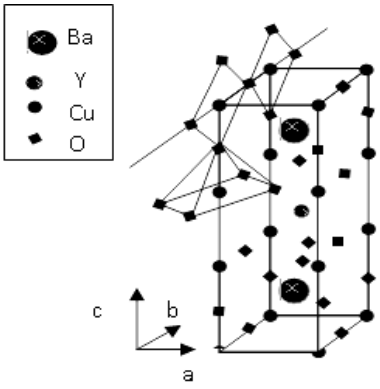

Fig. 1. The crystal structure of YBaCuO

Table 1
Qualitative characteristics of substrates

Substrate material	Qualitative characteristics			
	Lattice matching	CTE matching	Microwave properties Reconciliation of KTR Microwave properties Quality of HTSC	HTSF quality
Lanthanum aluminate $LaAlO_3$	Excellent	Excellent	Good	Excellent
Lanthanum gallate $LaGaO_3$	Excellent	Excellent	Good	Good
Strontium titanate $SrTiO_3$	Excellent	Excellent	Very bad	Excellent
Substrate material	**Qualitative characteristics**			
	Lattice matching	**CTE matching**	**Microwave properties**	**HTSF quality**
neodymium gallate	Good	Excellent	Very bad	Excellent
Nd GaO_3	Bad	Good	Good	Bad
Zirconium dioxide stabilized with yttrium ZrO_2; Y_2O_3	Bad	Bad	Excellent	Bad
Sapphire Al_2O_3	Bad	Very bad	Excellent	Very bad

To obtain epitaxial HTSFs one can use single crystals which unit cell parameters are close to the corresponding parameters of HTSFs, or they differ approximately by a factor of two. In the first case, the crystallographic directions of the HTSF <110> lie along the directions of the <110> type of substrate and the error can be considered relative to the value of "a"/Y_2 of the substrate [4]. For superconductor electronics and microwave technology, both monocrystalline and polycrystalline films are required. In the first case, it is necessary to achieve a high-quality epitaxial fusion of a high-temperature superconductor film with a substrate by adjusting the lattice parameters of the substrate material and its thermal expansion coefficient to the corresponding value of these parameters for HTSF.

In the second case, the cracks and pores formed as a result of the difference in the lattice parameter and the CTE of the substrate material and HTSF are, as it were, closed, "healed" due to the chaotic distribution of the crystallites forming the polycrystalline film [5].

For the Y-Ba-Cu-O compound, which has lattice parameters (**Fig. 1**), a=0.38; b=0.39 and c=1.17 nm, one of the most suitable materials is strontium titanate (a_0=0.39 nm), with which the discrepancy with the parameter "a" is 2 %, and between "c" in YBaCuO and "c" in $SrTiO_3$ – 2 %. It is this circumstance that explains the wide use of substrates from $SrTiO_3$ (**Table 1**) for obtaining high-quality YBaCuO films. The $YBa_2Cu_3O_7$ films on the $SrTiO_3$ substrate have a very close

structure, resulting in a high ordering of the crystals in the films, in which the "c" axis is usually perpendicular to the substrate plane and, as a consequence, high values of jc (up to 5×10^6 A/cm) and small ΔT (1 K) [5, 7, 10–14].

High dielectric permittivity (**Table 1**) significantly limits the use of $SrTiO_3$, especially in microwave devices.

In addition, it should be borne in mind that when high-temperature treatment (annealing) is separated from $SrTiO_3$ strontium and replaces barium in $YBa_2Cu_3O_7$, decreasing the value of Δt_{pd}.

Studies [11-16] have shown that substrates made from $LaAlO_3$ significantly exceed all other substrates (Si, MgO, $SrTiO_3$, $LaGaO_3$) in Tc, jc, the interaction of the film with the substrate, the consistency of lattice and film constants, CTE, losses of microwave.

It can be concluded that for the creation of a high-temperature superconductor in a test sample it is possible to use a substrate of $LaAlO_3$ on which the $YBa_2Cu_3O_7$ film is deposited.

2. 2. Methods of making contacts for microstrip HTSFs

The problem of obtaining stable low-resistance contacts to HTSFs has two characteristic features. The first is a high current density (up to 5×10^6 A/cm^2), which can only be obtained in the HTSFs if the contact has a low transition resistance. Although, from a different point of view, the high chemical activity of HTSF causes the oxidation of metal contacts and the formation of a dielectric layer at the HTSF-metal interface. In addition, often the HTSF near-surface layer is dielectric even in the process of obtaining films as a result of a violation of stoichiometry in it or a crystal structure. Therefore, just before deposition on the surface of the HTSF-metal (usually Ag and Au), it is necessary to remove the near-surface dielectric layer or to restore in it somehow superconductivity.

In practice, ionic purification in inert gas plasma (more often argon) is used, but the thickness of the nonsuperconducting surface layer decreases, however, purification does not completely destroy gases, since structural changes occur with a depth of up to 4 nm (Cu-O bonds breakdown and oxygen diffusion). Cleaning in oxygen plasma causes a smaller change, but the films are very critical to the cleaning regime (the duration of the process, the angle of incidence of ions on the surface). Purification by removal of the surface layer of the HTSF material is also accompanied by destruction of the superconducting properties of the surface. Consequently, the surface of HTSF is a very unstable formation, and therefore it is necessary to protect it with films of other materials immediately after application. However, a very limited number of materials can be used for this purpose.

Most metals enter into chemical reactions with the HTSF material, causing the superconducting properties of near-surface layers of the HTSF to break down and to oxidize in the materials in contact with it. There are only a limited number of materials: Ag, Au, Pt, Ir, Ru, Rh, Pd, Os, Hg, which oxides have a lower binding energy than Cu-O. Only with the deposition of Ag and Au on the surface of YBaCuO does not form an oxide film, in all other cases an oxide film with a thickness of 4 nm for Cu and up to 14 nm for Al appears. The process of oxidation of materials is accompanied by the destruction of superconductivity and the formation of a semiconductor surface layer 2–5 nm in thickness.

Of all the currently known methods of obtaining ohmic contacts, two are the most suitable. In the first of these, before the deposition of Ag or Au, the surfaces of HTSFs are purified from the nonsuperconducting phase by ion sputtering. In the second method, YBaCuO films are grown in the presence of oxygen and annealed at T=850 °C and a high rate of temperature increase, while Au precipitates at T=20 °C immediately after cooling the YBaCuO film without violating the vacuum. The minimum achieved resistance of the interface of HTSF – normal metal is 10^{-10} Ω cm^2 [6].

2. 3. The main technological methods of applying HTSF onto the substrate

For the production of high-temperature superconducting films, in fact, the entire arsenal of available methods is used, but those that are organically fit into the general production cycle of production are most promising for use in industrial production. Such methods at the moment are laser and magnetron sputtering. Laser sputtering is perhaps the most flexible method of preparing

HTSFs. Spray can be almost any of the composition of the target. Quite the high cost of equipment is paid off by its efficiency and ease of control of the process. Another advantage is the possibility of using the same technique for profiling the surface.

In **Fig. 2** of [4, 8] is presented in a generalized form the scheme of the experimental equipment used for laser deposition of HTSF materials. The radiation from the laser, as a rule, at an angle to the surface, is focused on the target surface inside the vacuum volume. The sprayed material is deposited onto the heated substrate.

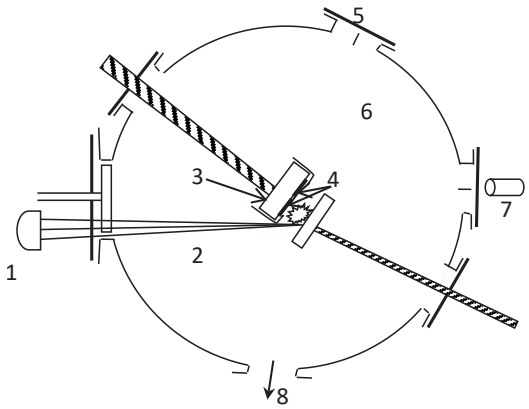

Fig. 2. Scheme of the equipment used for laser spraying of high-temperature superconducting material: 1 − lens; 2 − laser beam; 3 − heater; 4 − substrates; 5 − gas; 6 − rotating target; 7 − pyrometer; 8 − pumping out

Precipitation can be conducted both in a vacuum and in an atmosphere of a certain composition [8−10].

One of the drawbacks of the laser sputtering method is the presence of microdroplets in the laser torch. If the cluster particles containing dozens and hundreds of molecules contribute to the preservation of the stoichiometric composition and do not disturb the morphology of the surface of the films, the microdroplets, depositing on the surface, make it rough, cause various irregularities, and, in general, reduce the quality of the films. To avoid (or at least reduce) the impact of microdroplets on the surface of films, different screens are used [11−14]. The nature of laser ablation has been studied in sufficient detail in many works [11−13]. The heat treatment regimes are also studied in detail. Still, it is perhaps impossible to draw up complete recommendations on the production of films by laser sputtering. Sputtering conditions are very different both for the laser part (energy and power density, wavelength, focal spot size), and for other parameters (chamber pressure, substrate temperature, distance from the target). Nevertheless, the technology of obtaining films by the laser method is very popular, since all these parameters easily vary and allow to quickly find the optimum at which good films are obtained. Single-crystal films with high critical characteristics are obtained by a laser method. The use of lasers, as already noted, is also attractive because it is simultaneously possible to use laser radiation for other purposes. Fast high-temperature laser annealing is used [10], irradiation of the substrate during the sputtering with the same laser radiation [14], which is used for sputtering the target, lasers use to apply films of a certain pattern.

Another method of obtaining HTSFs is magnetron sputtering, for which magnetron sputtering systems (MSS) are used (**Fig. 3**).

Magnetron sputtering systems are essentially diode systems (**Fig. 3**), in which the interaction of electric and magnetic fields in combination with the shape of the sputtered target surface creates a configuration of magnetic traps for electrons, in which the electron drift currents are self-locked.

As a result, three maxima coincide in the MSS [4, 5]:

− the electron energy distribution function;

− the number of ionization acts that create one electron per unit of the path of its directed movement;

− the number of electrons knocked out by one ion from the target.

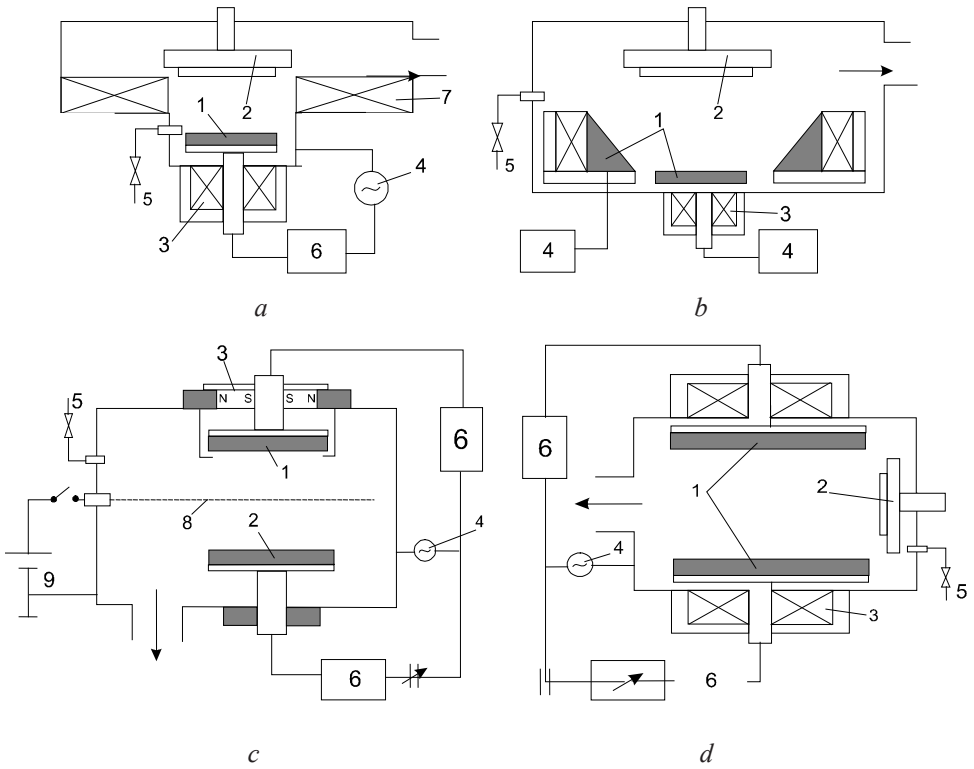

Fig. 3. MSS constructive options. *a, b, c, d* – options for depositing films: 1 – spraying target; 2 – substrate holder; 3 – magnetic system; 4 – power supply; 5 – gas supply system; 6 – matching device; 7 – additional magnetic system; 8 – mesh electrode; 9 – displacement source

The main MSS advantages, providing the possibility of their wide industrial use, are: higher energy efficiency of the process compared to SS of diode and triode types, and hence a higher rate of precipitation of the films.

The fact is that in MSS the high efficiency of the plasma formation process due to the presence of a magnetic field is combined with a high sputtering coefficient at an ion energy of 400−500 eV, which is characteristic for MSS;

− obtaining the required stoichiometry while simultaneously sputtering several targets by controlling the power supplied to each of the targets;

− the possibility of controlling the sputtering zone as a result of the use of several independent magnetic systems;

− the possibility of changing the structure and properties of films due to simultaneous sputtering of several targets with different velocities, changing the pressure and composition of the gaseous medium (percentage of Ar and O_2), the bias potential on the substrate, and other methods;

− low porosity and high adhesion of films even at small thicknesses;

− a lower (in comparison with conventional diode SS) radiation and thermal effects on the structures being processed and the possibility of its further reduction during the thermalization of the deposition process;

− inversion of the process, which makes it possible to use MSS for both preliminary cleaning (etching) of substrates, and for deposition of a wide class of materials;

− the versatility of the process, allowing in a single vacuum cycle to deposit on the substrate films of virtually any materials and compatibility of the process with other operations of the technological cycle of production of integrated circuits.

During the last decade, there have been intensive development and improvement of MSSs, typical design variants of which are presented in **Fig. 3**.

The laser method is much more reliable, provides a high deposition rate (<50 nm/min) and a stoichimetric composition of the resulting film without the use of complex instrumentation. How-

ever, it does not provide the proper level of quality of films with a thickness of less than 1 μm. To create such films, the magnetron sputtering method is most suitable.

To create a superconducting protective MA, the magnetron sputtering method is used [16].

3. Experimental study of the superconducting HTSF element

The article presents experimental studies of the obtained protective device based on high-temperature superconductors [16].

1. HTSF transient characteristics.

2. HTSF pulse characteristics of the limiter.

3. Time to restore the superconducting state after the action of a powerful pulse on the protective device.

4. Amplitude-frequency characteristics of the protective device in the superconducting state.

5. Characteristics of the electrical strength of a protective device based on HTSF.

The measurements are carried out for a superconducting sample − a high-temperature superconducting film ($YBa_2Cu_3O_7$) 0.1 μm thick deposited on the substrate ($LaAlO_3$) by the coaxial line РК-5. Contact of HTSF with the residential coaxial cable is carried out using vacuum or magnetron sputtered gold on a part of the film in contact with the holder.

When testing prototype models of protective devices, the following devices are used (**Fig. 4**):

− shaper of pulses И1-7;

− power supply Б5-50;

− oscilloscope С7-13, С8-14;

− measuring instrument Р4-11;

− generator Г3-34;

− recorder Н307.

3. 1. Transient characteristics of protective device

The transient characteristics of an HTSF-protective device (PD), that is, the dependence of the output voltage on the load from the input, are removed when a pulsed and sinusoidal voltage is applied.

Schemes for measuring transient characteristics are shown in **Fig. 5**. A voltage pulse with amplitude up to 130 V and a duration of t_i=45 ns is supplied from the generator И1-7 to a matched load of 50 Ω and a voltage divider formed by the HTSF sample under study and a load resistance R_l=50 Ω simulating the input resistance of the receiving electronics.

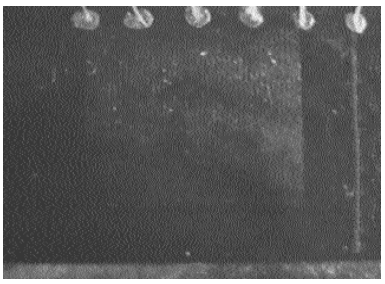

a

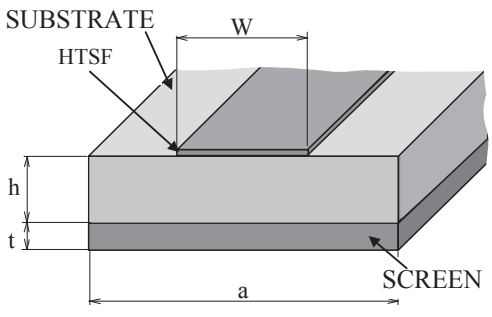

b

Fig. 4. HTSF PD in a microstrip antenna: *a* – PD appearance; *b* – PD structure

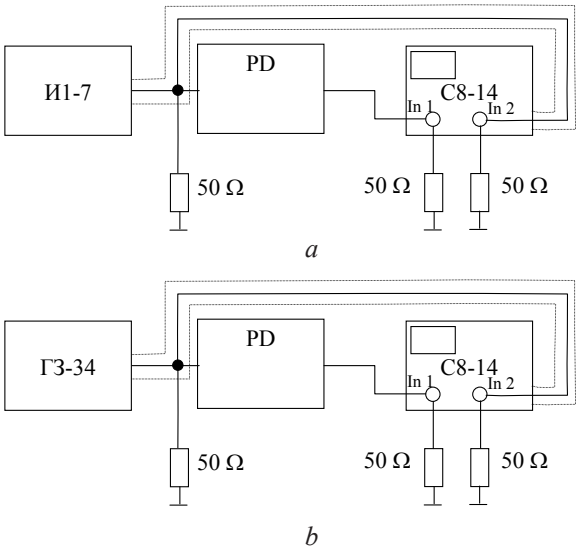

Fig. 5. Schemes for measuring transient characteristics: *a* − pulse; *b* − harmonic regime

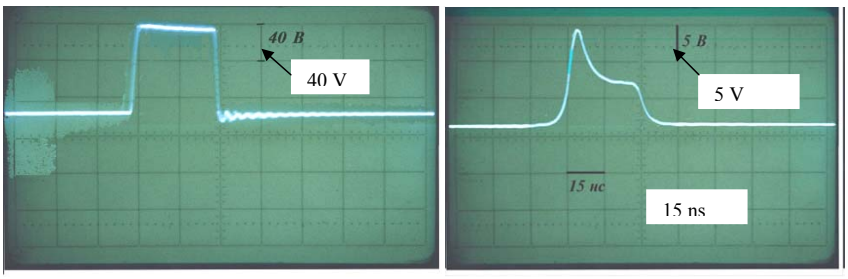

a *b*

Fig. 6. Oscillograms of the generator voltage pulses at the coordinated load and the output voltage for the HTSF protective device at room temperature: *a* – input pulse; *b* – output pulse

The parameters of the pulses of the input and output voltages are measured with an oscilloscope C8-14, which has a rise time of the transient response t_r<7 ns, which is clearly seen from a typical oscillogram of the generator voltage pulse on the coordinated load shown in **Fig. 6**.

Similarly, the characteristics are removed when a sinusoidal voltage of 100 kHz and amplitude of 0.1 to 11 V is applied from the Г3-34 generator.

The experimental sample is obtained by the magnetron method on a common substrate of $LaAlO_3$.

The investigated protective device has the following initial characteristics [1–3]:

– resistance at room temperature R_2 = 100kΩ;

– resistance near the superconducting transition (at T> Tc) Ro=(50) kΩ;

– contact resistance $r_{con}=10^{-2}$ Ω [12, 16].

It should be noted that there is a parasitic capacitance (C) (**Fig. 7**) between the screen and the superconductor. This capacitance has little effect on the propagation of the signal at low frequencies (Xc=1/jωC in **Fig. 7**), but turns out to be significant at high frequencies of the transmitted signal (**Fig. 6** – distortion of the front and the decay of the pulse).

The transient characteristics of the sample and the corresponding coefficients are shown in **Fig. 8, 9**. These characteristics are measured for the time instant t_0=50 ns on the plane vertex of the pulse (quasi-stationary mode). It can be seen from the above dependences that the superconducting state is observed for the amplitudes of the input pulses u_{in}<10 V, after which the amplitude gradually falls to 7−8 V.

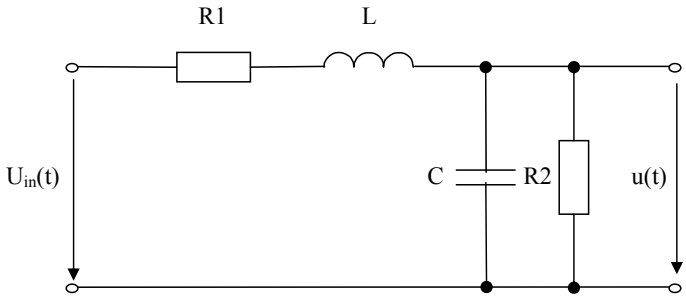

Fig. 7. Equivalent connection circuit of HTSF PD

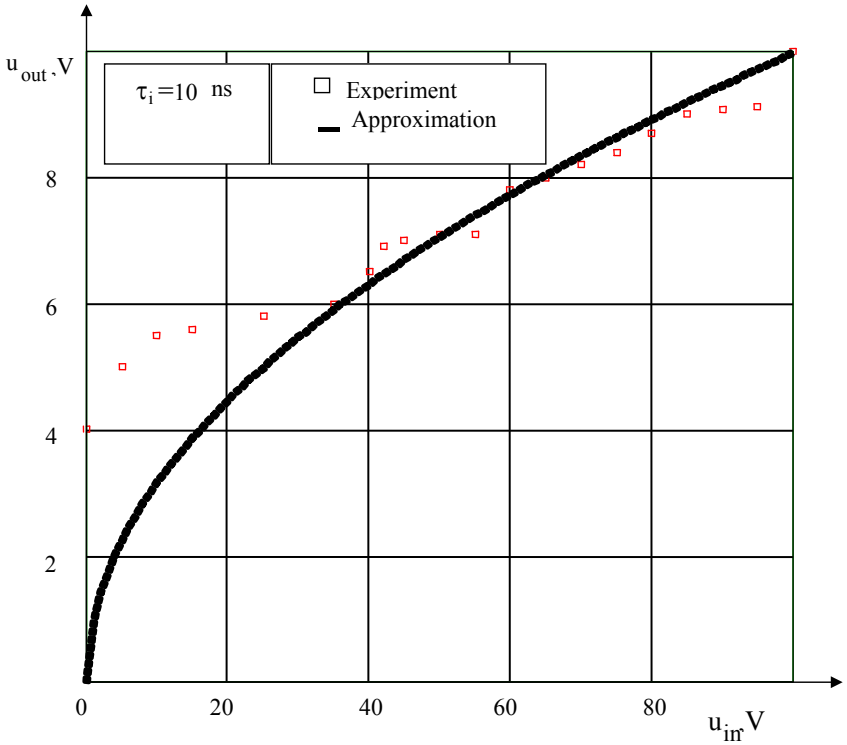

Fig. 8. Transient coefficient of a HTSF-based protective device under the action of a sinusoidal signal

This value u_{in} corresponds to the current in the circuit corresponding to the current density through the sample, which approximately coincides with the critical current density of the superconductor.

The absence of a sharp break in the transient characteristic when a critical current is reached is associated with a transient region of current superconductivity, which means that the restoration of the nonsuperconducting resistance of the sample occurs at low currents, and this transient process has no connection with the inertia of the superconducting properties of the film.

As the cross section of the superconductor decreases, the current reaches its critical value much faster. In this case, the amplitude of signals transmitted without significant distortion is less. If the input effect (voltage) has a sinusoidal form, then the considered PD also limits the level of the output voltage at the level of 9 V.

The superconducting state is observed for u_{in}=1−7 V, after which the permanent screening begins to the value u_{in}=8 V.

Consequently, the limiter based on HTSF transmits without distortion voltage signals up to 8 V, and if this level is exceeded, the output voltage does not exceed 12 V (**Fig. 6**).

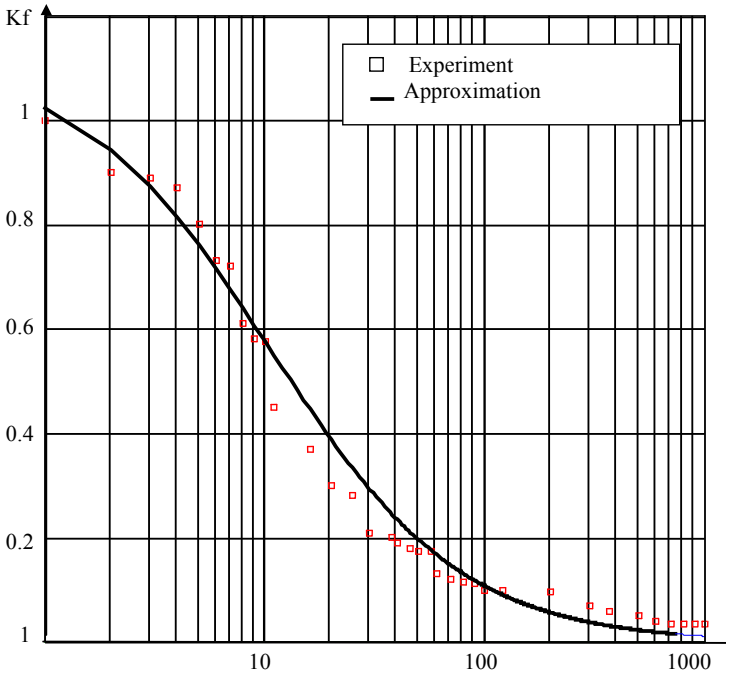

Fig. 9. Transient coefficient of a HTSF-based protective device under the pulse action

3. 2. Transient characteristics of pulse processes

Fig. 10 shows the oscillograms of the transient processes obtained for average amplitudes of the input pulses (H307 is used). When comparing (**Fig. 10**) the figures show that the rise time of the front of the output pulse will be 10 ns (5 %). This distortion of the front is related to the parasitic integrating capacitance of the sample on the common bus (**Fig. 7**), which is actually equivalent to the capacity of the sample with respect to an infinitely remote point having a zero potential.

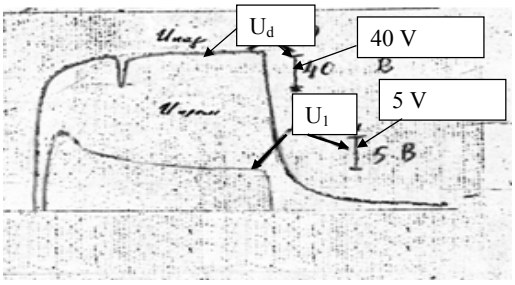

Fig. 10. Oscillogram of transient processes with average amplitude of input pulses (U_d)
Note: U_d – input pulse. U_l – output pulse

Since the dielectric constant of the substrate, its diameter and the length of the conductor l satisfy the relation $\varepsilon_n/l<<1$, the effect of the substrate on the capacitance of the conductor is insignificant. Knowledge of the value of the integrating capacitance makes it possible to determine the value of the input voltage $u_{in}(t) - U_m(e^{-a_1 t} - e^{-a_2 t})$. (**Fig. 10**) when the voltage is applied (**Fig. 7**)

$$u(t) = Um(A_1 e^{-a_1 t} + A_2 e^{-a_2 t} + A_3 e^{-\alpha t} sh(\alpha_1 t) + A_4 e^{-\alpha t} ch(\alpha_1 t), \quad (2)$$

where

$$\left.\begin{aligned} A_1 &= \frac{R_2}{K_1}; A_2 = \frac{R_2}{K_2} \\ A_3 &= (a_2 - a_1)K_4\left[R_2^2 LC\left[R_2 LC(a_1 + a_2)(CR_2R_1 + L) + K_5\right]\right] \\ A_4 &= (a_2 - a_1)R_2 K(-R_2 LCa_1 - R_2 LCa_2 + R_2 CR_1 + L) \end{aligned}\right\}, \quad (3)$$

where

$$\left.\begin{aligned} K_1 &= R_1 - a_1 R_2^2 C - a_1 L + a_1^2 R_2 LC + R_2 \\ K_2 &= -a_2 R_2 R_1 C - a_2 L + a_2^2 R_2 LC + R_1 + R_2 \\ K_3 &= \sqrt{4CLR_2^2 + 2R_1 R_2 CL - R_1^2 R_2^2 C^2 - L^2} \\ K_4 &= \frac{K}{-K_3\sqrt{R_2^2 L^2 C^2}} \\ K_5 &= -R_2^2 C^2 R_1^2 + 2R_2^2 LC - L^2 - 2R_2^2 L^2 C^2 a_1 a_2 \\ K &= 1/K_1 K_2 ; \alpha_1 = \frac{1}{2}\frac{K_3}{\sqrt{R2^2 L^2 C^2}} ; \alpha = \frac{1}{2}\frac{(R_1 R_2 C + L)}{R_2 LC} \end{aligned}\right\}, \quad (4)$$

R_1 – the resistance of the HTSF sample in the n-state, R_2 – the load resistance, (**Fig. 11**)

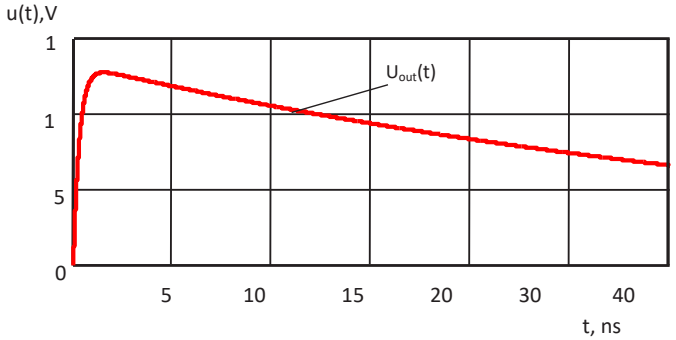

Fig. 11. Calculated dependence of output voltage on time

The shape of the diagram (**Fig. 11**) of this voltage approximately (error up to 8 %) [6] coincides with the oscillogram in **Fig. 6**. Analysis (4) and data in **Fig. 6** shows that in this case:

$$U_{out\ max} / U_{in\ max} = 1{,}4 \times 10^{-1}, \quad (6)$$

Consequently, the integrating capacitance phenomenon is decisive in determining the shape of the output voltage [6, 16].

Experimental studies have confirmed that the transition of a high-temperature superconductor (the main element of the prototype PD sample) from a superconducting state to a nonconducting state (i. e., the PD switching process) lasts less than 1 ns and the output voltage does not exceed 12 V.

3. 3. Time to restore the PD superconducting state

A comparison of the results obtained with each other (**Fig. 10**) shows that in the case of sufficiently large amplitudes of the input voltage pulses (more than 100 V) there is no decay of the plane vertex of the output pulse during operation of the memory with a superconducting element (HTSF). This effect [9, 16] due to the heating of the superconductor by a flowing current, as a result of which its resistance increases in comparison with the resistance in the region of the critical point of the transition. An increase in the amplitude of the input voltage by a factor of 20 will lead to a similar drop in the amplitude of the output voltage. Consequently, the question of restoring the superconducting state after passing through powerful pulses is arises.

The scheme for measuring the recovery time is shown in **Fig. 12**. From the generator И1-7 to the input of the circuit, along with a powerful pulse, the pulse of the generator Г5-60 with amplitude of 0.15 V is delayed. The outputs of the generators are separated by pulsed diodes. In the superconductivity regime, the amplitude of the output pulse from the second generator should be 0.12 V.

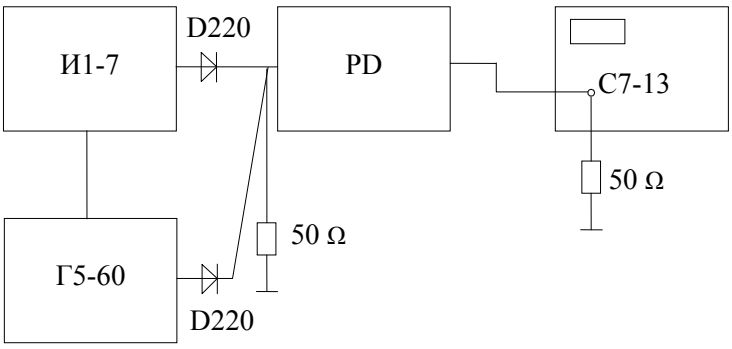

Fig. 12. Scheme for measuring the recovery time of the superconducting state of HTSF device

The smaller amplitudes of the output pulse mean that the sample did not completely transfer to the superconducting state. Changing the delay of the pulse of the second generator, it is possible to determine the interval during which the superconductivity is restored. The smallest interval of pulse separation time is 0.45 ns. Complete restoration of superconductivity occurs in 3 μs, which corresponds to calculations (an error of 0.15 %) [16].

As the amplitude of the input pulse increases, the recovery time will increase. If assume that this growth is directly proportional to the electric power output (and this is the worst case, when the pulse is fed to a high-temperature superconductor element with a duration of 100 ns and amplitude of 40 kV, the recovery time does not exceed 5 μs).

3. 4. Frequency responce of a superconducting PD

Measurement of the frequency response is carried out with the help of the device P4-11. The measurement scheme is shown in **Fig. 13**. To determine the transmission coefficient, the value of the output signal of the limiter is given to the value of the input signal.

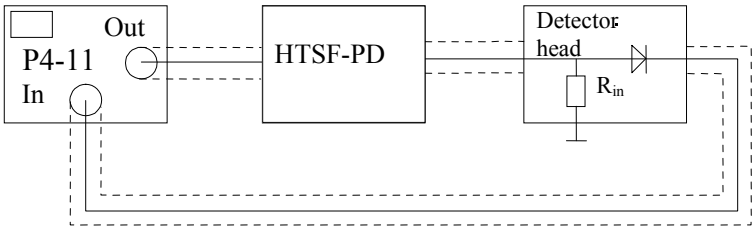

Fig. 13. The scheme of HTSF-PD frequence response measurement

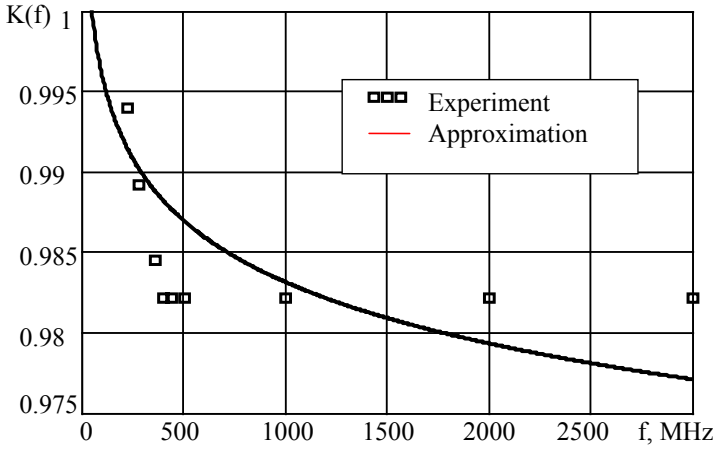

Fig. 14. Frequence response of HTSF-based PD

The measurement is carried out in the 0÷2500 MHz band and for two characteristic measurement areas of the input signals: u_{1in}=40 mV, when the sample is in the superconducting state and u_{2in}=400 mV, when the sample begins to limit the amplitude.

Let's first consider the small amplitudes of the input signal, which make it possible to judge the undistorted frequence responce of the superconducting limiter. **Fig. 14** shows the frequency response of the HTSF-microstrip line [16]. It follows from the results of the research that the considered limiter based on the superconducting coaxial-waveguide junction is normal (the coefficient is 1 with a thousandth of an error) operates over a wide range of operating frequencies (studied in the range from 100 MHz to 3 GHz). In carrying out all the above experimental studies, there is no organic breakdown of the HTSF sample. Physical destruction means the electrical breakdown of the superconducting strip on the screen. The absence of breakdown is explained by the fact that, with a high resistance of an HTSF microstrip in its normal state, even with kilowatt amplitudes of input voltage pulses, the current through the sample does not reach the limiting values (10−30 mA), and also because the nitrogen in which the sample is located is itself a dielectric ($E_{cnitrogen} > E_{cair.}$).

4. Approximation of the results of experimental studies

As a result of the experimental studies, an array of values of the input and output voltages of the memory are determined, which collectively represent the transfer characteristic of HTSF-based PD in the case of a powerful pulse signal (**Fig. 8, 9, 14**). The type of approximating functions of the obtained experimental data is determined in the work (**Table 2**). The "APPROX" mathematical package is used to select functions (**Fig. 15, 16**):

Table 2

A set of functions offered by "APPROX" (**Fig. 15**) for approximating the results of the experiment shown in **Fig. 8**

No.	Approximating function	Deviation from experiment, V	
		Standard	Maximum
1	$y = \sqrt{1.01 \cdot x}$	0.288	4
2	$y = 53.227 \cdot 10^{-3} x + 4.506$	0.049462	−0.506
3	$y = 45{,}32 \cdot 10^{-6} x^2 + 48 \cdot 10^{-3} x + 4.578$	0.048705	−0.578
4	$y = \sqrt{3.1 \cdot 10^{-3} x^2 + 0.46 \cdot x + 20{,}2}$	0.049521	0.490
5	$\mathrm{Ln}(24{,}9\times10^{-6})T4(x)-0.252T2(x)+ +21{,}4\times T1(x)+54{,}7T0(x)$	0.0345	0.369

Note: $x=u_{in}(t)$, $y=u_{out}(t)$,$Ti(x)=\cos(\pi/N)\times i$

By the same principle "APPROX" program found expressions that mathematically can describe the result of the experiment in **Fig. 9** are presented in **Table 3** and **Fig. 16**. From **Fig. 15** and **Table 2** it follows that function (5) gives the minimum standard deviation (SD), function (3) has also a small SD.

However, the accuracy of the formulas is verified by substituting new experimental points, and it turned out that function (3) most accurately describes the transientr characteristic of HTSF-based PD under pulse action.

Thus, in **Table 4** the results of the function selection by "APPROX" program that most accurately summarizes the results of the experimental studies presented in **Fig. 8, 9**.

Table 3

A set of functions proposed by "APPROX" for approximating the results of the experiment presented in Fig. 9

No.	Approximating function	Deviation from experiment, V	
		Standard	Maximum
1	$y = \sqrt{0.994/x}$	0.019	–0.253
2	$y = e^{-0.281 \cdot \ln(x)}$	0.024	–0.239
3	$y = 1/(0.084 \cdot T1(x) + 0.892 \cdot T0(x))$	0.007	–0.100
4	$y = (-46.47 \cdot 10^{-6} \cdot T2(x) + 0.0945 \cdot T1(x) + +0.854 \cdot T0(x))^{-1}$	0.0065	–0.081

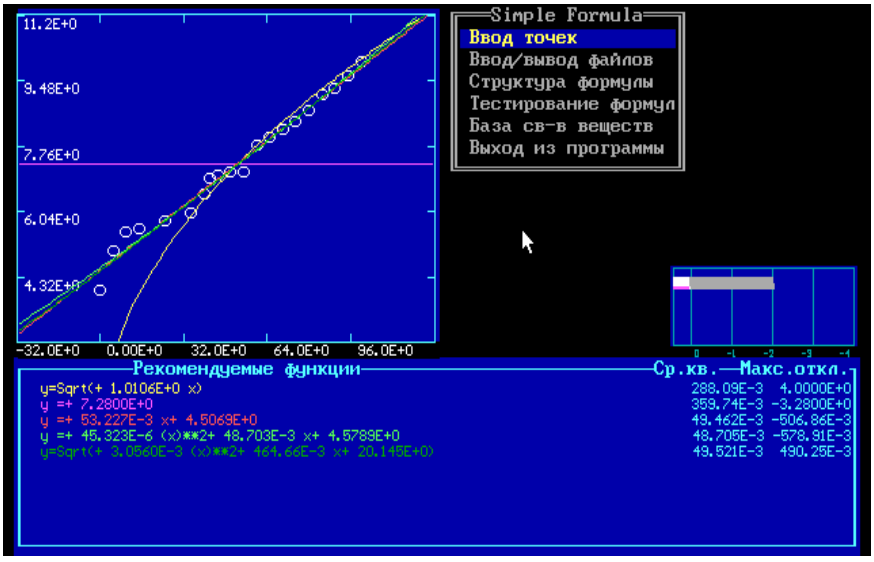

Fig. 15. The results of determining the type of approximating functions of the experiment results by "APPROX" program in **Fig. 8** (also in **Table 2**)

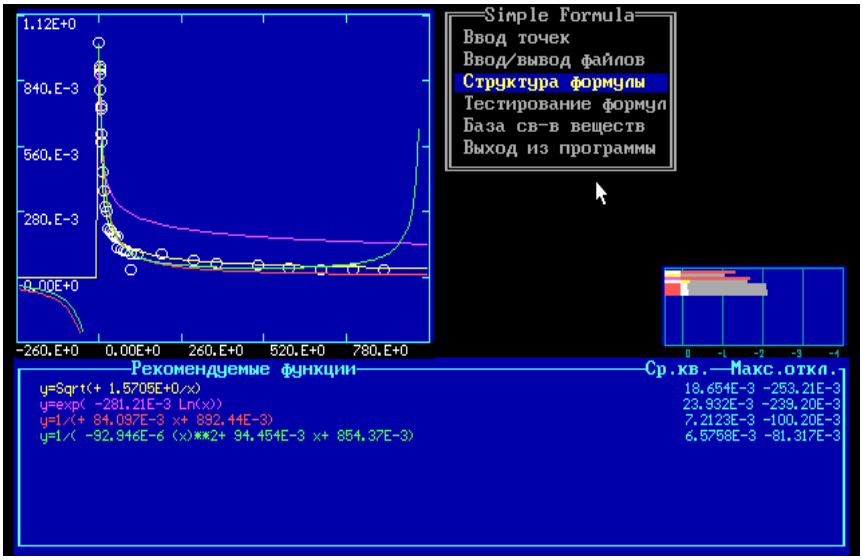

Fig. 16. The results of determining the type of approximating functions (**Table 3**) of the experiment results by "APPROX" program in **Fig. 9**

Table 4

Functions approximating the experimental results

Figure number from experiment	The functions that most accurately approximate the experimental results	Deviation from experiment, V	
		Standard	Maximum
Fig. 8	$y = 45{,}32 \cdot 10^{-6} x^2 + 48 \cdot 10^{-3} x + 4.57$	0.048705	–0.578
Fig. 9	$y = 1/(0.084 \cdot T1(x) + 0.892 \cdot T0(x))$	0.007	–0.100

Note: $x=u_{in}(t)$, $y=u_{out}(t)$,$Ti(x)=\cos(\pi/N)\times i$

The obtained results of the program are checked by means of MATHCAD

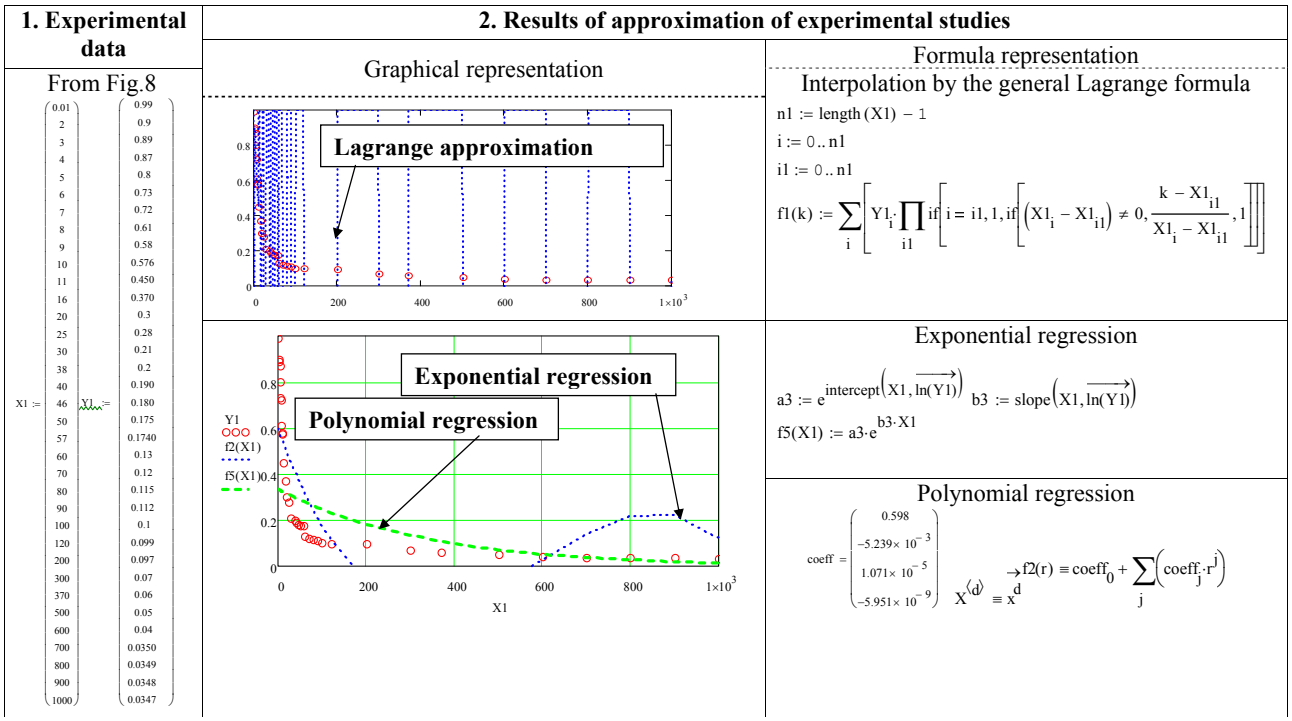

Fig. 17. Processing of the experimental results (Fig. 8) in MathCAD

5. Conclusions

− the manufactured sample of the microstrip antenna protective device (HTSF 1 micron deposited by a magnetron or laser method on a substrate (Al_2O_3 or $SrTiO_3$)) does not disturb the wave structure upon arrival and transmission;

− the superconducting protective device allows to reduce the signal level of high power 1000 times (up to 1 volts);

− the recovery time of a superconducting protective device after an electromagnetic failure does not exceed 3 μs;

− APPROX package for testing formulas (**Fig. 15, Table 2**) is possible to determine that the most accurate approximation of the experimental results (**Fig. 8, 9**) with the help of functions $y_1 = 45{,}32 \cdot 10^{-6} x^2 + 48 \cdot 10^{-3} x + 4.57$ $y_2 = 1/(0.084 \cdot T1(x) + 0.892 \cdot T0(x))$ (**Table 4**). In the MathCAD14.0 mathematical package, the accuracy of the "APPROX" package is confirmed (**Fig. 16**), (error 0.15);

− the use of high-temperature superconducting antenna devices will exclude the possibility of electromagnetic damage to its semiconductor elements, **Fig. 17**.

References

[1] Fyk, A. I. (2015). Modelirovanie elektromagnitnogo polya v pryamougolnom volnovode s sverkhprovodyashhim sterzhnem. Mezhdunarodnyi Nauchnyi Institut "Educatio". Ezhemesyachnyi nauchnyi zhurnal, 6 (13 (2)), 17–21.

[2] Berezinec, V. M., Kucher, D. B., Fyk, A. I. (1997). Skorost fazovogo S–N perexoda sverxprovodyashhego zashhitnogo ustroistva. Nauchno-texnicheskii sbornik KhVU, 1 (5), 77–81.

[3] Berezinec, V. M., Kucher, D. B. (1993). Vliyanie sverkhpovodyashhego vysokotemperaturnogo plenochnogo elementa na prokhozhdenie signalov cherez fidernye linii svyazi. Informacionnye sistemy. Kharkiv: ANU, 29–32.

[4] Konkov, K. E., Molchanov, A. S. (1992). Poluchenie plenok Y–Ba–Cu–O metodom lazernogo napyleniya. Sverkhprovodimost: fizika, khimiya, tekhnika, 5 (4), 46–48.

[5] Vendik, O. G. (Ed.) (1991). High-Tc Superconductors: Physical Principis of Microwave Applications. Leningrad, l48.

[6] Berezinec, V. M., Kucher, D. B., Fyk, A. I. (1999). Eksperimentalnoe issledovanie koaksialno-volnovodnogo perekhoda. Radioelektronika i informatika, 4, 21–24.

[7] Sobol, E. N. et. al. (1990). Obzory po vysokotemperaturnoi sverkhprovodimosti. Moscow: MCNTI, 3, 94–131.

[8] Grigorev, G. Yu. (1990). Tekhnologiya polucheniya i nekotorye svoistva VTSP–plenok. Obzory po VTSP. Moscow: MCNTI, 2, 25–69

[9] Crabtree, G. W., Kwok, W. K., Welp, U., Burriel, R., Claus, H., Vandervoort, K. G., Liu, J. Z. (1988). The upper critical field of high temperature superconductors. Journal of Magnetism and Magnetic Materials, 76-77, 547–551. doi: 10.1016/0304-8853(88)90483-0

[10] Bendre, D. (1990). High-temperature superconductors. Solid state communications, 73 (5), 345.

[11] Simon, R. (1989). High-temperature superconductors for microelectronics. Solid State Technol, 3 (9), 141–146.

[12] Talvacchio, J. (1989). Electrical contact to superconductors. IEEE Transactions on Components, Hybrids, and Manufacturing Technology, 12 (1), 21–31. doi: 10.1109/33.19008

[13] Ohya, S., Kobayashi, K., Hirabayshi, V. (1989). High–temperature superconductors. Japanese Journal of Applied Physics, 28 (6), 978–980.

[14] Kolinsky, P. V., May, P., Harrison, M. R., Miller, P., Jedamzik, D. (1989). Substrate-temperature dependence of thin films of BiSrCaCuO deposited by the laser ablation method. Superconductor Science and Technology, 1 (6), 333–335. doi: 10.1088/0953-2048/1/6/013

[15] Shirman, Ya. D. (1959). Radiovolnovody i obyomnye rezonatory. Moscow: Sovetskoe radio, 370.

[16] Berezinec, V. M., Kucher, D. B. (1993). Rezultaty eksperimentalnogo issledovaniya amplitudno-chastotnykh kharakteristik i vremeni vosstanovleniya sverkhprovodyashhego sostoyaniya ogranichitelya na osnove VTSP. Tematicheskiy nauchno-tekhnicheskii sbornik KhVU, 339, 31–34.